Petroleum 11 (2025) 41–55

Contents lists available at ScienceDirect

Petroleum

journal homepage: www.keaipublishing.com/en/journals/petlm

Full Length Article

Effect of potential determining ions on sulfonated polyacrylamide behavior during smart water-polymer injection into carbonate reservoirs

Seyed Masoud Ghalamizade Elyaderani, Amir Hossein Saeedi Dehaghani *, Javad Razavinezhad, Rasoul Tanhay Choshali

Department of Petroleum Engineering, Faculty of Chemical Engineering, Tarbiat Modares University, Tehran, Iran

A R T I C L E I N F O

Article history:
Received 11 July 2024
Received in revised form
18 October 2024
Accepted 20 December 2024

Keywords:
Enhanced oil recovery
Smart water-polymer solution
Potential determining ions
Polymer adsorption
Zeta potential
Viscosity
Calcite-coated micromodel

A B S T R A C T

In low salinity polymer flooding (LSPF), an advanced hybrid method for enhanced oil recovery (EOR), less attention has been given to the impacts of potential determining ions on polymer behavior in carbonate reservoirs. Therefore, seawaters spiked with divalent ions were used with sulfonated polyacrylamide (SPAM) polymer to investigate the effects of potential determining ions on SPAM performance in wettability alteration, polymer adsorption, carbonate surface charge, viscosity enhancement, emulsion type, and oil recovery. Among divalent anions and cations, only excess amounts of Mg^{2+} in a smart water-polymer solution could alter the wettability from oil-wet to neutral-wet and make the rock/brine zeta potential positive. Additionally, higher SPAM adsorption onto carbonate surfaces was observed as Mg^{2+} concentration was doubled, driven by interactions between sulfonate groups ($-SO_3^-$) and the positively charged rock surface. Conversely, excess SO_4^{2-} impeded interactions between $-SO_3^-$ and positively charged carbonate rock species, reducing SPAM adsorption. At 5000 ppm SPAM concentration, excess divalent ions increased solution viscosity due to the shielding effect, with the highest viscosity achieved by doubling Mg^{2+} concentration. However, at 10,000 ppm SPAM concentration, only SO_4^{2-} improved viscosity, while Ca^{2+} and Mg^{2+} reduced the viscosity of smart water-polymer solutions. As for emulsions produced by smart water-polymer solutions, the presence of SPAM in smart water led to the production of water-in-oil (W/O) emulsions and increased the mean droplet size of water droplets due to the salt-out effect. According to the results obtained from calcite-coated micromodel flooding experiments, the ultimate oil recovery for SW + SPAM (5000 ppm) was 34.2%. Also, a two-fold increase in the Mg^{2+} concentration rose the oil recovery by 6.5%.

© 2024 Southwest Petroleum University. Publishing services by Elsevier B.V. on behalf of KeAi Communications Co. Ltd. This is an open access article under the CC BY-NC-ND license (http://creativecommons.org/licenses/by-nc-nd/4.0/).

1. Introduction

Carbonate reservoirs are well known for their heterogeneity and wettability conditions [1–4]. Indeed, the wetting state of these reservoirs is mainly oil-wet, inducing negative capillary pressure [5,6]. Also, high-permeable fractures are connected to low-permeable matrix blocks, making the carbonate reservoirs more complex [7,8]. Owing to these two attributes, the injected water cannot overcome the capillary pressure when conventional water flooding is applied. In this regard, the fluid flow from the fractures into the matrix blocks does not take place, and considerable amounts of oil are trapped in the porous media. Therefore, it is paramount to explore an injection fluid that outperforms the water flooding in oil production from carbonate reservoirs. More specifically, following primary and secondary recovery methods, approximately 30% of the original oil in place (OOIP) can be produced [9,10]. As a result, nearly two-thirds of OOIP remains in the pores and throats of porous spaces. To extract the bypassed/unswept oil, tertiary or enhanced oil recovery (EOR) methods are used as a key strategy to boost oil production [11,12].

Numerous chemicals are typically used in EOR, including alkaline, polymer, surfactant, nanoparticle, etc [13–20]. Although these materials can boost the amount of oil recovery to a great extent,

* Corresponding author.
E-mail address: asaeedi@modares.ac.ir (A.H. Saeedi Dehaghani).
Peer review under the responsibility of Editorial Office of Petroleum.

https://doi.org/10.1016/j.petlm.2024.12.002
2405-6561/© 2024 Southwest Petroleum University. Publishing services by Elsevier B.V. on behalf of KeAi Communications Co. Ltd. This is an open access article under the CC BY-NC-ND license (http://creativecommons.org/licenses/by-nc-nd/4.0/).

they may pose environmental threats. Additionally, chemical-EOR techniques are not feasible when it comes to economic issues. In recent years, tuned seawater flooding has caught the attention of myriad researchers [21,22]. This is because not only is it less detrimental to the environment, but also it is cost-effective [23,24]. Tuned seawater is classified as low salinity water and smart water, obtained by reducing the brine salinity and increasing the ionic composition of the brine, respectively [25,26]. Based on bench-scale and field pilot studies, it has been proved that altering the brine composition of seawater can raise oil recovery in carbonate reservoirs [27,28]. When it is utilized as an injected fluid, an equilibrium associated with the crude oil-brine-carbonate rock system is disrupted [29–31]. Consequently, the injected fluid can move from the high-permeable fractures and enter low-permeable matrix blocks by overcoming capillary pressures, increasing the amount of oil recovery. According to the literature, the chief mechanism of tuned seawater flooding is wettability alteration; however, there is no agreement on the reasons that account for alteration in the wetting state of carbonate rock. In general, rock dissolution, multi-component ion exchange, and double layer expansion may be responsible for the wettability alteration by tuned seawater flooding [32–37].

Due to tuned seawater flooding, the microscopic sweep efficiency can be enhanced. Nevertheless, since having a viscosity lower than crude oil, smart water or low salinity water flooding leads to inadequate macroscopic displacement efficiency, and the carbonate reservoirs may not be sufficiently swept. Researchers have recently added water-soluble polymers to tuned seawater flooding to tackle the poor sweep efficiency problem. Indeed, adding polymer can improve water viscosity and reduce mobility ratio, thereby leading to a more piston-like displacement. Thus, viscous fingering is minimized, and more amount of oil is produced [38,39].

Multiple studies have been performed on the different aspects of tuned seawater-polymer flooding. In terms of wettability alteration, using partially hydrolyzed polyacrylamide (HPAM) and two different brines, Souayeh et al. [40] reported that the homogeneous oil-wet calcite surface could become strongly water-wet as polymer concentration and its molecular weight (MW) increased. They also revealed that the lowest contact angle was achieved in HPAM solution containing 100-time diluted formation water. Li et al. [41] prepared sulfonated polyacrylamide (SPAM) with high MW in the seawater at both ambient and elevated temperatures, indicating that the oil-wet carbonate rock surface was rendered neutral-wet at two different polymer concentrations, and the contact angle further decreased as SPAM concentration increased. Moreover, Alsofi et al. [42] reported that adding SPAM at 2000 ppm to 10-time diluted seawater positively affected wettability alteration, making the carbonate rock surface neutral-wet. However, they found that the presence of polymer in the diluted seawater could not decrease the contact angle when the calcite surface in place of carbonate reservoir rock was used. Utilizing core samples mainly composed of calcite ($\geq$99%) and low salinity brines comprised of NaCl/$CaCl_2$ or NaCl/Na_2SO_4 along with 300 ppm of HPAM, Lee et al. [43] concluded that the wettability of samples could change from oil-wet to water-wet as low salinity-HPAM solutions were flooded, and SO_4^{2-} could lead to more contact angle reduction compared to Ca^{2+}. Also, Amiri et al. [44] studied the wettability alteration of oil-wet quartz chips when HPAM was applied at various concentrations in seawater, 10-time diluted seawater, and double-concentrated seawater. They showed that increasing HPAM concentration in seawater and double-concentrated seawater could not change the quartz wettability. In contrast, they observed that only the combination of 10-time diluted seawater and HPAM at 1000 ppm led to neutral-wet condition. As can be observed, the mentioned previous studies have not comprehensively examined the influence of potential determining ions and polymers on wettability alteration of carbonate rocks during smart water-polymer flooding. Previous studies primarily focused on investigating the impacts of polymer concentration, dilution degree, and MW on wettability alteration. Moreover, in the study conducted by Lee et al. [43], the brines consisted of only two salts, which differs significantly from the injection brines used in EOR processes that typically comprise a blend of salts, such as NaCl, $CaCl_2$, $MgCl_2$, and Na_2SO_4. Consequently, a clear understanding of how divalent ions, in conjunction with polymer, can detach oil molecules and render carbonate rocks more water-wet remains elusive. This knowledge gap is particularly significant since one method of creating a smart water solution involves adjusting divalent ion concentration in seawater or diluted seawater.

Regarding polymer adsorption during tuned seawater-polymer flooding, Kakati et al. [45] observed that low salinity water reduced the amount of polyacrylamide (PAM) adsorbed on the sand surface as opposed to seawater. In addition, Lee et al. [43] used simplified low salinity brines with a total dissolved solid of 6000 ppm and 300 ppm of HPAM to explore the polymer adsorption during core flooding tests. They showed that increasing concentration of Ca^{2+} or SO_4^{2-} in low salinity-HPAM flooding could decrease polymer adsorption on the calcite surface according to values of mobility and permeability reduction factors. Additionally, Unsal et al. [46] utilized HPAM with two different brines and reported that polymer retention declined with decreasing salinity from 6392 to 785. On the contrary, Souayeh et al. [40] obtained the opposite result and observed that low salinity brines resulted in an increase in polymer adsorption. They reported that HPAM adsorption on calcite surface increased to 27.8 and 50.3 mg/g as formation brine was diluted 10 and 100 times, respectively. The reviewed studies mainly focused on the effects of salinity and HPAM polymer concentration on adsorption, and the study done by Lee et al. [43] did not directly measure HPAM adsorption using low salinity brines containing only two salts. Therefore, the specific interactions between potential-determining ions and SPAM polymers require deeper investigation to discern the adsorption phenomenon of polymer on carbonate rocks. This could provide valuable insights into optimizing smart water-polymer flooding processes for enhanced oil recovery.

With regard to viscosity enhancement, Unsal et al. [46] compared the viscosity of HPAM solutions in high salinity and low salinity brines. They showed that low salinity brine led to a higher viscosity than high salinity brine at low shear rates and vice versa. They further demonstrated that introducing Ca^{2+} and Na^{+} into a low salinity-polymer solution decreased the viscosity. Alsofi et al. [42] reported that the SPAM viscosity was improved in low salinity brine at different concentrations when seawater was diluted 10 times. In addition, Kakati et al. [45] evaluated the viscosity of PAM solutions at 70°C using varied low salinity brines. They observed that 10-time diluted seawater resulted in a 36% enhancement in the viscosity at a shear rate of 18 s^{-1}. Likewise, Alfazazi et al. [47] found that the viscosity of solutions containing HPAM and low salinity brines could be improved by reducing the salinity of seawater. Lee et al. [43] examined the impact of low salinity brines comprised of NaCl, Na_2SO_4, and $CaCl_2$ on the viscosity of HPAM solutions. In this regard, they showed that the presence of Ca^{2+} could decrease the viscosity slightly, although increasing the concentration of SO_4^{2-} marginally improved the viscosity of the low salinity-HPAM solution. Tahir et al. [48] also reported that the viscosity of HPAM solution increased as Na_2SO_4 concentration was doubled in 10-time diluted seawater. Moreover, Hernández et al. [49] studied four high MW polymers with diluted seawater solutions to determine the amount of polymer required to reach a target viscosity. With decreasing brine salinity, they showed that less amount of polymer

was required to achieve the target viscosity. It should be noted that Lee et al. [43] explored the impact of Ca^{2+} and SO_4^{2-} on the performance of low salinity-polymer flooding; nevertheless, they utilized brines that were only composed of NaCl/$CaCl_2$ or NaCl/Na_2SO_4. Indeed, seawater is comprised of numerous salts, and the influence of potential determining ions in the presence of various monovalent and divalent ions should be investigated to elucidate their actual roles. Also, Tahir et al. [48] only examined the viscosity enhancement as the excess amount of SO_4^{2-} was present in low salinity-polymer solutions. Therefore, there is still much to be discovered about how potential determining ions affect the viscosity of tuned seawater-polymer solutions, and this knowledge can aid in tailoring brine compositions for maximum viscosity enhancement.

Concerning rock surface charge in tuned seawater-polymer solutions, Souayeh et al. [40] reported that increasing HPAM concentration in low salinity brines induced more negative charges on the calcite surface. Lee et al. [43] performed zeta potential experiments using low salinity brines with 300 ppm of HPAM and concluded that the calcite surface had a negative charge in the presence of SO_4^{2-} and Ca^{2+}. They also showed that increasing concentrations of SO_4^{2-} and Ca^{2+} resulted in an increase and a decrease in the absolute zeta potential values, respectively. Furthermore, Amiri et al. [44] measured the silica nanoparticle/brine zeta potentials and used seawater, 10-time diluted seawater, and double-concentrated seawater alongside HPAM. They revealed that HPAM in different brines could react with silica surfaces and reduce its negative charges, making the zeta potential more positive. Past studies have revealed a research gap concerning the influence of SPAM polymers and their interplay with potential determining ions on carbonate rock surface charge. While previous research has centered around the effects of HPAM polymers and certain potential determining ions on calcite surface charge, as well as SPAM polymers and diluted seawater on silica surface charge, a more comprehensive understanding of SPAM-ion interactions and their impact on carbonate surface charge is necessary.

Relating to oil recovery improvement owing to tuned seawater-polymer flooding, using core flooding experiments in sandstone, Abdullahi et al. [50] reported that the ultimate oil recovery rose by 7.3% when low salinity brine was utilized in HPAM solution instead of high salinity brine. Moreover, Souayeh et al. [40] conducted forced imbibition into limestone cores at 75°C and reported that low salinity-HPAM and high salinity-HPAM injections increased the oil recovery to 71% and 69%, respectively. Piñerez Torrijos et al. [51] performed low salinity-HPAM flooding in sandstone cores as secondary and tertiary stages to examine the oil recovery factor. According to their results, the combination of HPAM and diluted seawater could be only efficient in enhancing the amount of oil recovery when utilized in the tertiary mode, increasing oil recovery by 22%. Furthermore, Alsofi et al. [42] found that 10-time diluted seawater-SPAM injection into carbonate reservoirs outperformed either low salinity water flooding or polymer flooding. At room temperature (25°C), Lee et al. [43], performed flooding experiments into the calcite cores, revealing that increasing SO_4^{2-} concentration in simplified low salinity-HPAM polymer solution can yield additional oil recovery of 12.3%. It can be deduced from previous studies that there is a potential research gap regarding the lack of clarity on how potential determining ions in smart water-polymer solutions may affect oil production. This knowledge would enable the development of more effective and tailored strategies for enhanced oil recovery during smart water-polymer flooding.

Overall, the potential of engineered/smart water, obtained by increasing potential determining ion concentration in seawater, remains largely unexplored in tuned seawater-polymer flooding. Specifically, little attention has been given to the combination of engineered seawater and SPAM polymer for enhancing oil recovery from carbonate reservoirs. Additionally, the roles of potential determining ions in wettability alteration, polymer adsorption, viscosity of solutions, and carbonate rock surface charge need further clarification when combining smart water and SPAM polymer. In other words, the effects of Ca^{2+}, Mg^{2+}, and SO_4^{2-} ions on various EOR aspects in the presence of SPAM polymers require further investigation. This study aims to bridge knowledge gaps in smart water-polymer flooding for carbonate reservoirs, focusing on the impacts of potential determining ions. The primary goal is to unveil the underlying mechanisms when combining seawater enriched with potential determining ions and SPAM polymer for EOR purposes. Additionally, this study investigates the influence of these ions on SPAM behavior during rock/brine interactions. Ultimately, it seeks to determine which potential determining ion in seawater can positively affect the SPAM solution for EOR applications. To this end, different smart waters with two polymer concentrations were prepared, and contact angle, viscosity, adsorption, and rock/brine zeta potential, and emulsion formation experiments were conducted. In addition, a calcite-coated micromodel was applied to assess the ultimate oil recovery by smart water-polymer flooding and investigate the phenomena at the pore scale. It is worth mentioning that previous studies only utilized core flooding to evaluate oil recovery enhancement during tuned seawater-polymer flooding. Simply put, no study has so far flooded tuned seawater-polymer solution into a calcite-coated micromodel for the EOR purpose. Fig. 1 illustrates the schematic of experimental procedure used in this study.

2. Material and methods

2.1. Oil

A heavy crude oil sample used in this research was taken from one of the Iranian oil fields located southwest of Iran. In order to remove solid particles as well as water and gases dissolved in the oil sample, we first centrifuged the oil and then filtered it through the filter paper (5 mm). Table 1 presents the properties of crude oil.

2.2. Brine

Different salts, provided by Merck (Germany), were utilized to prepare seawater resembling Persian Gulf seawater with a total dissolved salinity (TDS) of 47,208 ppm. Also, five smart water solutions were synthesized, including SW2Mg, SW2Ca, SW2SO4, SW2Mg_2SO4, and SW2Mg_2Ca. For example, SW2Mg signifies that the concentration of $MgCl_2$ in smart water is 2 times the concentration of $MgCl_2$ in seawater; SW2Mg_2SO_4 denotes that both concentrations of $MgCl_2$ and Na_2SO_4 have doubled as compared to their concentrations in seawater. It is important to note that in the context of this study, the term "smart water" refers to seawater that has been modified by increasing the concentration of potential determining ions. Table 2 shows the composition of formation brine (FB), seawater (SW), and smart water solutions alongside ionic strength values. In this study, the base fluid was distilled water with surface tension and pH of 71.8 ± 0.7 mN/m and 7.15, respectively. In addition, for preparing smart waters, the procedure introduced by Maghsoudian et al. [34] was applied. In this regard,

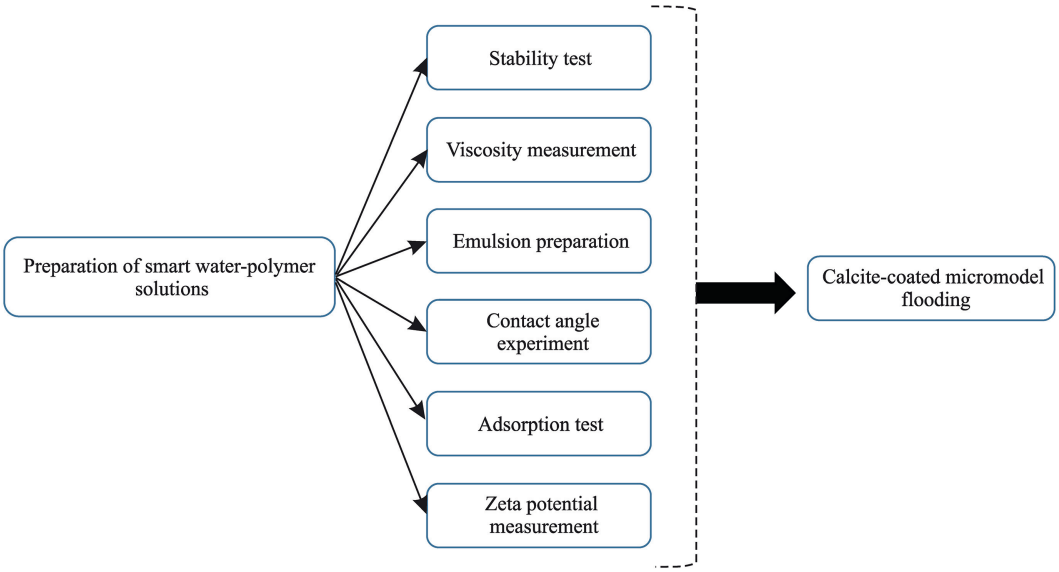

Fig. 1. Schematic of experimental procedure.

Table 1
Crude oil properties.

Viscosity (cp) @ 25 °C	Density (gr/cc)	TBN (mg KOH/g oil)	TAN (mg KOH/g oil)	Asphaltene (wt%)	Resins (wt%)	Aromatics (wt%)	Saturates (wt%)
530	0.93	1.2	0.8	14.1	15.1	36.7	34

Table 2
Composition of various brines.

Brine	Na^+ (ppm)	Ca^{2+} (ppm)	Mg^{2+} (ppm)	SO_4^{2-}(ppm)	K^+ (ppm)	HCO_3^-(ppm)	Cl^- (ppm)	Ionic strength (mmol/l)	Total dissolved solids (ppm)
Formation brine = FB	69,813.8	17910.9	786.1	0	1804	0	121,706.2	3938	212,021
Seawater = SW	11,999.9	439.8	3484	3110.25	453.3	166.35	27,554.4	1028	47,208
SW2Mg	11,999.9	439.8	6968	3110.25	453.3	166.35	37,719.4	1457	60,857
SW2Ca	11,999.9	879.6	3484	3110.25	453.3	166.35	28,332.6	1061	48,426
$SW2SO_4$	13,488.65	439.8	3484	6220.5	453.3	166.35	27,554.4	1124	51,807
$SW2Mg_2Ca$	11,999.9	879.6	6968	3110.25	453.3	166.35	38,497.6	1490	62,075
$SW2Mg_2SO_4$	13,488.65	439.8	6968	6220.5	453.3	166.35	37,719.4	1553	65,456

the order of adding salt to the distilled water was as follows to increase the stability of varied smart waters:

$$CaCl_2 \rightarrow MgCl_2 \rightarrow NaCl \rightarrow KCl \rightarrow Na_2SO_4 \rightarrow NaHCO_3$$

2.3. Polymer

A SPAM polymer with a MW of 2 million daltons and a sulfonation degree of 25% was used in this study, purchased from SNF Floerger (France). Fig. 2 illustrates the molecular structure of the SPAM polymer. As can be seen, there are negatively charged sulfonate groups on the SPAM backbones. According to the literature [52], SPAM, as opposed to HPAM, is more salt tolerant, and its viscosity is less susceptible to divalent ions. Thus, we selected this type of polymer for our research. To prepare smart water-polymer solutions, two SPAM concentrations, 5000 and 10,000 ppm were chosen. These selections are because this SPAM is categorized as a low MW polymer. Thus, it should be utilized at high concentrations to effectively improve the viscosity of injected fluid so as to increase heavy oil recovery.

To prepare the smart water-polymer solution, the desired smart water was prepared by dissolving the required salts in a beaker containing distilled water. Next, SPAM powder was slowly added to the desired smart water while simultaneously being stirred using a magnetic stirrer at 700 rev/min for 10 min at room temperature. This speed of the stirrer was selected to avert fish-eye formation and polymer agglomeration, which could have a negative effect on the complete hydration of SPAM. Then, the solution was stirred for additional 48 h at 300 rev/min to obtain the well-dissolved SPAM solution. It should be noted that the stability of all smart-water polymer solutions was checked by using a qualitative method at two different temperatures. As shown in Fig. S1 (See supporting information), no precipitation or color change can be seen, illustrating that the hybrid solutions have stability after 45 days.

2.4. Rock properties and preparation

In order to conduct the contact angle test, we utilized a carbonate core taken from an outcrop in the southern regions of Iran. Table 3 presents the results of the X-ray fluorescence (XRF) analysis. As can be seen, CaO makes up a more significant percentage of the sample (above 50%), inferring that the core used in this study was a carbonate rock.

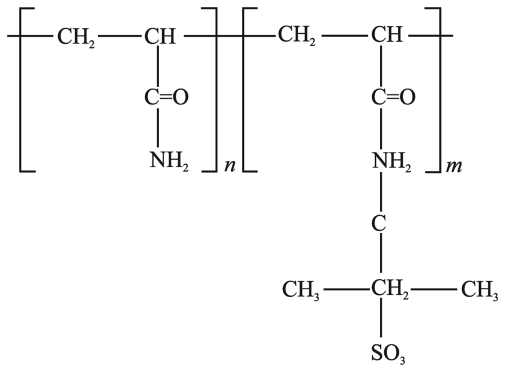

Fig. 2. Molecular structure of SPAM [52].

To prepare the samples for the tests, we obtained thin sections with a thickness of about 2 mm after placing the core in a special chamber and cutting it. Following the thin sections being polished, they were washed using toluene (Dr. Mojallali Industrial Chemical Complex Co., ≥99%) and methanol (Merck, ≥99.9%) in Soxhlet extraction. The sections were subsequently placed in an ultrasonic bath for 2 h and then dried in an oven for one day to clean the rock surface from contamination. Next, for two days, the sections were saturated with FB. Eventually, to make the sections oil-wet, they were immersed in the crude oil for 30 days at 90°C. As can been from Fig. S2 (See supporting information), the rock chips were made oil-wet.

2.5. Contact angle measurements

Oil-wet thin sections were aged in the smart water-polymer solutions for 60 days at 70°C to determine the effects of potential determining ions and SPAM on wettability alteration. The sessile drop technique, as shown in Fig. 3, was also adopted to measure the contact angle values. Precisely, the treated thin section was put in a glass cell filled with distilled water, and a drop of oil was placed on the surface of the thin section by a needle. After 5 min, when the drop reached equilibrium on the surface, it was photographed under a microscope. Finally, using image analysis software (Digimizer), we obtained contact angle value between the oil and the rock surface. Then, the contact angle between water and the rock surface was determined using the following equation, where θ_{oil} is the oil-surface contact angle, and θ_{water} is the water-surface contact angle.

$$\theta_{water} = 180^{\circ} - \theta_{oil} \tag{1}$$

If θ_{water} is between 0° and 30°, the carbonate surface is strongly water-wet, and if θ_{water} is between 30° and 75°, the carbonate surface is weakly water-wet. Neutral-wetness occurs when θ_{water} is between 75° and 105°, and oil-wetness occurs when θ_{water} exceeds 105° [54]. It should be noted that θ_{water} was reported for each brine as a contact angle value to assess the water-wetness of carbonate surface. Each contact angle test was conducted three times, and the average of these tests was reported as the final value to minimize error. Also, all contact angle tests were performed at 26°C.

2.6. Zeta potential measurement

The zeta potential of rock/brine was measured by Zetasizer (ZEN 3600, UK) to evaluate the impact of smart waters along with SPAM on the surface charge of carbonate rock. In this respect, 0.125 g of carbonate powders with an average size of 50 μm were mixed with 20 mL of solution in a beaker for each experiment. Afterward, the beaker was shaken at atmospheric conditions using a shaker for 72 h. After that, desired time was given to have a clear suspension with the deposited powders at the bottom. Then, a syringe with a fine needle was applied to separate the suspension from the powders, and the separated fluid was filtered to eliminate rock particles. In the final stage, the filtered solution was put in the vessel of the Zetasizer to assess the zeta potential values. It should be pointed out that each test related to zeta potential was performed three times at 28°C, and an average value was reported.

2.7. Static adsorption experiment

In this study, static adsorption tests were performed to examine the SPAM adsorption on the carbonate rock in different smart waters. In this regard, 2 g of crushed rock and 20 mL of smart water were mixed in a test tube. Then, the test tube was shaken at room temperature using a shaker for 72 h to reach the maximum polymer adsorption. Afterward, the test tube was left still for several hours until a transparent smart water-polymer solution was obtained, and powder particles settled at the bottom. Next, a sample was taken from the transparent solution, and the SPAM concentration following adsorption was determined by utilizing UV–Vis spectrophotometer (Optizen 3220UV, Korea) at a wavelength of 230 nm. It should be noted that this wavelength was chosen since the maximum absorbance of smart water-polymer solutions occurred. A calibration curve was obtained from known polymer concentrations to find unknown polymer concentrations in smart water-SPAM solutions. Eventually, the following equation was employed to calculate the adsorption of SPAM on the carbonate rock, where q displays the SPAM adsorption (mg/g), C_i is the initial SPAM concentration (mg/L), C_f denotes the final SPAM concentration (mg/L) measured by UV–Vis spectrophotometer, V shows the volume of smart water-polymer solution (l), and W signifies the weight of crushed rock (g).

$$q = \frac{V \times \left(C_i - C_f\right)}{W} \tag{2}$$

2.8. Microfluidic experiment

A glass micromodel that became calcite-coated was utilized to witness the effect of smart water-polymer flooding on the amount of oil recovery and discover pore scale phenomena. Table 4 illustrates the physical features of the calcite-coated micromodel.

The glass micromodel was naturally made up of silica (SiO_2). In other words, it did not bear a resemblance to carbonate rock. Therefore, we made the glass micromodel calcite-coated to have porous media resembling carbonate rock. As described by Wang et al. [55] and Ghalamizade Elyadrani et al. [29], we used a method

Table 3
XRF of carbonate rock.

Formula	SiO_2	Al_2O_3	Fe_2O_3	CaO	Na_2O	K_2O	MgO	TiO_2	MnO	P_2O_5	SO_3	L.O.I
%	4.57	0.2	0.09	51.49	0.3	0.025	1.1	0.006	0.003	0.095	0.128	42.083

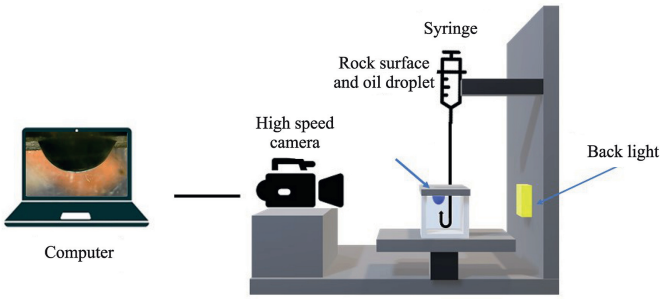

Fig. 3. Schematic of contact angle test.

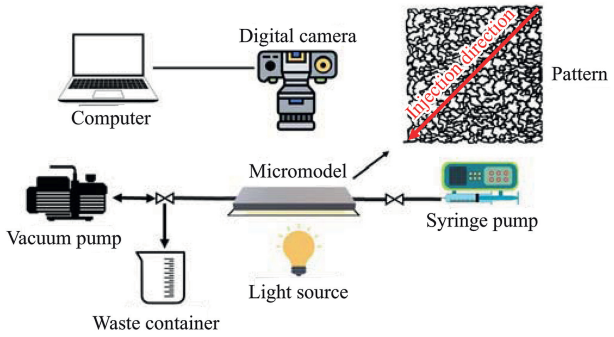

Fig. 4. Schematic of flooding setup with micromodel pattern.

in which nanocrystalline layers of $CaCO_3$ are formed on the pores and throats of micromodel. In this method, firstly, the micromodel was rinsed with a solution made of ammonium hydroxide (Merck, 28–30%) and hydrogen peroxide (Dr. Mojallali Industrial Chemical Complex Co., 35%). Next, 1 M sodium hydroxide solution was injected at a specified rate for 30 min, and distilled water was used to wash the micromodel after injection. A 20 mL solution was prepared by mixing chloroform (Merck, 99.8%) with distilled water in a 1:1 ratio. Then, a chloroform/silane solution was made by slowly adding 2 mL of N-(Trimethoxysilylpropyl)ethylenediamine (Gelest, 35% in water) to the prepared solution, and its pH value was adjusted to 1.5 by utilizing hydrochloric acid (Merck, 37%). Afterward, using a pump, the air was injected into the porous spaces of the micromodel after it was saturated with the chloroform/silane solution for 15 min, and this step was repeated three times. The 0.05 M $CaCl_2$ and ethanol (Scharlau, 99.9%) solutions were used to wash and clean the micromodel, followed by drying at 60°C. When the micromodel was cooled down, 0.05 M $CaCl_2$ was pumped into it and stayed for 10 min, followed by the air injection. Afterward, 0.05 M Na_2CO_3 solution was injected into the micromodel and remained for 10 min, and the air was then pumped into it to remove the solution. It is also noteworthy that the injections of $CaCl_2$ and Na_2CO_3 solutions were redone five times to ensure the adequate thickness of calcite in the pores and throats of micromodel. In the final stage, distilled water was pumped into the micromodel to wash it. Then, it was dried overnight at 60°C.

For seven days, to render the micromodel oil-wet, it was saturated with oil at 90°C. It should be noted that the micromodel was made oil-wet before each flooding test. Next, smart water-polymer flooding was performed in the oil-saturated micromodel, and the photos were shot at different intervals by a Canon 700D camera with a Canon EF 50 mm f/1.8 STM lens. Afterward, the amount of oil recovery was calculated using Adobe Photoshop CS6. A flow rate of 0.05 mL/h was used for each flooding experiment to preclude turbulence behavior in porous media [56]. Fig. 4 displays the schematic of the flooding setup and the micromodel pattern.

2.9. Rheological measurement

A rotational viscometer (Anton Paar QC viscometer, Germany) was applied to elucidate the effect of varied smart waters on the viscosity of SPAM solutions. In this respect, 18 mL of smart water-SPAM solution was poured into the special cup, and the viscosity was measured by inserting a CC27 spindle. It is worth mentioning that all the viscosities were captured at a constant shear rate of 1000 s^{-1}. Additionally, the viscosity measurement was carried out 5 times for each solution, and the average value was reported.

2.10. Emulsion preparation and droplet size measurement

Emulsification can play a crucial role in EOR and water treatment [57]. Thus, we examined the ability of hybrid fluids to produce emulsions. In this respect, oil was poured into a beaker. Then, smart water was added to the beaker drop by drop while stirred by a magnetic stirrer at 800 rpm for 60 min. Finally, the smart water and oil mixture was put in a test tube, and different samples were taken from the middle of the tube. Each emulsion sample was put in a glass slide, and a high-resolution microscope (USB Digital Microscope, China) took images from different parts of the slide. Afterward, Image J software was utilized to measure the mean droplet size for prepared water-in-oil (W/O) emulsion by analyzing the taken images. It should be noted that the smart water and oil were mixed in a volume ratio of 1:2. Also, for each smart water reported in Table 2, the emulsion was prepared three times, and the average value was reported as the mean droplet size.

3. Results and discussion

3.1. Impact of divalent ions on viscosity of smart water-polymer solution

Fig. 5 shows the viscosity of smart water-polymer solutions for two SPAM concentrations.

As can be seen, the viscosity of SW was found to be 6.8 cP at a SPAM concentration of 5000 ppm. Also, the viscosity for SW2Mg, SW2Ca, $SW2SO_4$, $SW2Mg_2SO_4$, and $SW2Mg_2Ca$ was 8.2, 7.7, 7.5, 7.5, and 6.9 cP, respectively. Obviously, viscosity increases slightly as divalent cations and anions concentrations are increased to 2 times of their initial concentrations in SW. This result is not in line with previous studies [43,46] showing that increasing Ca^{2+} and Mg^{2+} concentrations leads to a reduction in the polymer viscosity. Indeed, in this study, as 5000 ppm of SPAM was dissolved in seawater, all the intrinsic electrical charges on polymer molecules were neutralized by monovalent and divalent cations. Therefore, as the concentration of divalent ions increased, there were no electrical charges left that could be affected by the excess amount of Ca^{2+}, Mg^{2+}, and SO_4^{2-}. As a result, adding each divalent ion to the SW only marginally improved the solvent viscosity. In addition, this

Table 4
Micromodel properties.

Pore volume (cm^3)	Permeability (mD)	Porosity (%)	Length (cm)	Width (cm)	Average depth (cm)
0.25	920	41	6	6	0.005

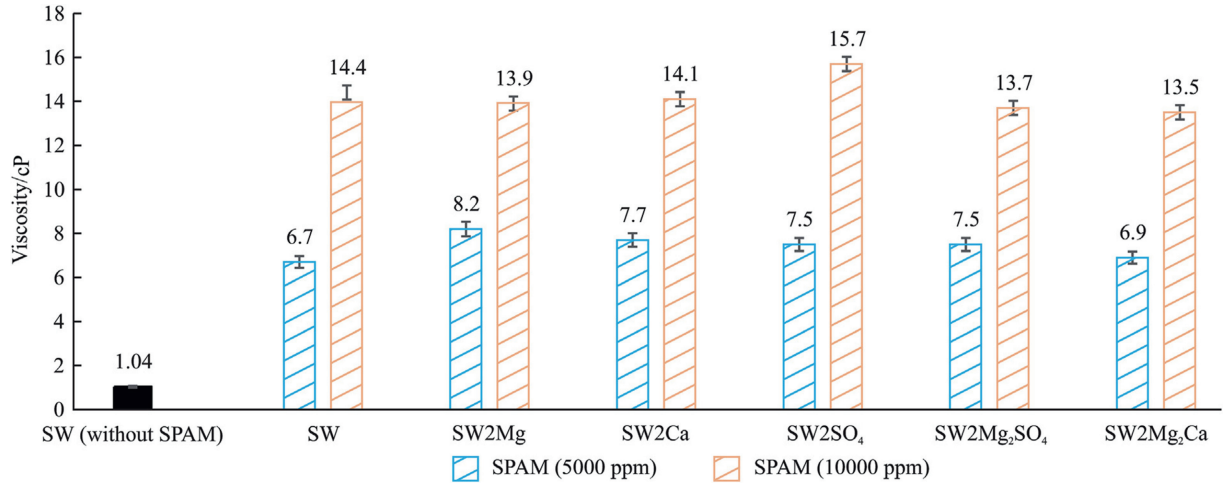

Fig. 5. Viscosity of different smart water-polymer solutions at a shear rate of 1000 s^{-1}.

marginal enhancement in the viscosities of SPAM solutions can be attributed to chain overlap and entanglements due to the high concentrations of divalent ions. In other words, the presence of Ca^{2+} and Mg^{2+} in the solution can neutralize negatively charged sulfonate groups of SPAM, resulting in a coiled conformation. The coiled chains can lead to entanglements and increased viscosity. This is because the reduction in electrostatic repulsion between different chains, also caused by divalent ions, allows the chains to approach each other more closely. This increased proximity promotes chain overlap and entanglements, thereby boosting the viscosity.

Among studied smart waters, SW2Mg resulted in a higher viscosity improvement. This is because the initial concentration of $MgCl_2$ in SW is relatively high (13,649 ppm). In other words, the concentration of Mg^{2+} is higher than that of Ca^{2+} and SO_4^{2-}; thus, more solvent viscosity enhancement can be observed when Mg^{2+} concentration is doubled in SW. In accordance with the present study, Rashidi et al. [53] revealed that increasing Na^{+} concentration beyond a specific salinity can contribute to a marginal rise in the viscosity of a solution containing high MW SPAM polymer.

However, according to Fig. 5, the viscosity of smart water-polymer solutions at 10,000 ppm SPAM concentration showed opposite results as the concentrations of divalent ions increased. The viscosity for SW was 14.3 cP, and a 2 times increase in the concentration of Ca^{2+}, Mg^{2+}, and SO_4^{2-} resulted in a viscosity of 14.1, 14.4, and 15.7 cP, respectively. It can be inferred that although the excess amount of SO_4^{2-} in smart water-polymer solution enhanced the viscosity, the rising concentration of Ca^{2+} and Mg^{2+} lightly declined the SPAM viscosity. In comparison with the viscosity results obtained by 5000 ppm polymer, all negative charges on the SPAM structure are not shielded by the cations in SW with 10,000 ppm polymer. Accordingly, the extra amount of divalent ions can have electrostatic interactions with the negatively charged sulfonate groups on the SPAM molecules. Thus, each divalent ion can affect the polymer viscosity.

Regarding divalent cations, when added to a smart water-polymer solution, Ca^{2+} or Mg^{2+} can electrostatically react with sulfonate groups to decrease the negative charges on the SPAM backbones. This reduction causes the SPAM chains to transform into spherical coils [58]. Consequently, SPAM molecules cannot remain extended since fewer negative charges are present on the polymer chains to repel each other, reducing the solution viscosity. Nevertheless, concerning divalent anions, the extra amount of SO_4^{2-} can contribute to an increase in the viscosity of the smart water-polymer solution. Indeed, SO_4^{2-} ions have a negative charge, and their presence near SPAM chains is likely to strengthen the repulsive forces between SPAM molecules. This, in turn, can boost the SPAM hydrodynamic volume, thereby increasing the viscosity of the smart water-polymer solution [59]. Also, as shown in Fig. 5, a 2 times increase in both concentrations of Ca^{2+} and Mg^{2+} in the presence of 10,000 ppm SPAM reduced the viscosity from 14.4 to 13.5 cP. This is due to the fact that more amounts of negatively charged sulfonate groups are bound to be neutralized with increasing divalent cations concentrations. In consequence, the shielding effect occurs, SPAM chains coil up, and the viscosity reduces [60,61]. Moreover, as the amounts of SO_4^{2-} and Mg^{2+} were doubled in the solution, the viscosity declined to 13.7 cP. Indeed, since the initial concentration of $MgCl_2$ (13,649 ppm) in seawater is higher than that of Na_2SO_4 (4599 ppm), the excess amount of Mg^{2+} suppresses the positive impact of SO_4^{2-} on viscosity enhancement.

3.2. Impact of divalent ions on wettability alteration of carbonate rock

Before conducting the contact angle test, we rendered the carbonate thin sections oil-wet. The average contact angle value for oil-wet rock chips was 159.9°, indicating that the wetting state of the thin sections became strongly oil-wet. Fig. 6 illustrates the contact angle values for different smart water-polymer solutions.

At SPAM concentration of 5000 ppm, the contact angle for SW, SW2Mg, SW2Ca, $SW2SO_4$, $SW2Mg_2SO_4$, and $SW2Mg_2Ca$ was 133.2°, 104.8°, 123.1°, 127.2°, 99.1°, and 115.5°, respectively. As evident, among divalent ions, only a 2 times increase in the concentration of Mg^{2+} could change the wettability to a neutral-wet condition. In other words, the excess amounts of Ca^{2+} and SO_4^{2-} did not alter the oil-wet wettability, although spiking their concentrations decreased the contact angle values. The superior performance of Mg^{2+} in reducing contact angles compared to Ca^{2+} and SO_4^{2-} can be attributed to the tendency of smaller ions to be more present at the rock/brine interface [62]. Ions with higher charge densities also enhance the solubility of surface-active agents at the rock/brine interface [63]. As shown in Table 5, Mg^{2+} possesses a smaller ionic radius and higher charge density, making it more effective in contact angle reduction. The smaller ionic radius of Mg^{2+} increases its likelihood of migrating from the water bulk to the rock/brine interface, while its higher charge density enables more effective interactions with oil molecules. These factors

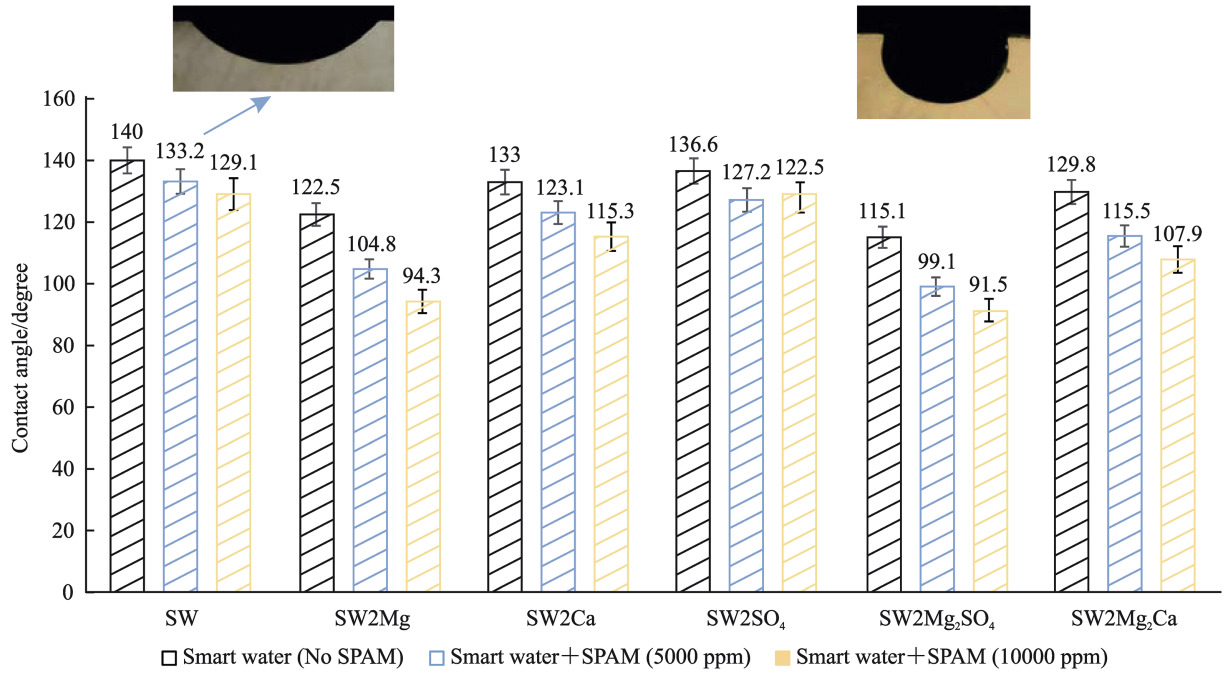

Fig. 6. Effect of different smart water-polymer solutions on contact angle values.

Table 5
Ionic radius and charge density of divalent ions.

Ion type	Ionic radius (nm)	Charge density (C/mm^3)
SO_4^{2-}	0.231	5
Ca^{2+}	0.100	52
Mg^{2+}	0.072	120

contribute to the detachment of oil molecules, thereby promoting a more water-wet state compared to Ca^{2+} and SO_4^{2-}.

In the case of increasing concentrations of two divalent ions simultaneously in smart water-polymer solutions, it is apparent that $SW2Mg_2SO_4$ has more capacity than $SW2Mg_2Ca$ to modify the carbonate rock wettability, making it neutral-wet. The lowest contact angle was obtained as the concentrations of Mg^{2+} and SO_4^{2-} were concurrently increased 2 times. In addition, as SPAM concentration rose to 10,000 ppm in SW, SW2Mg, SW2Ca, $SW2SO_4$, $SW2Mg_2SO_4$, and $SW2Mg_2Ca$, the contact angle values of 129.1°, 94.3°, 115.3°, 122.5°, 91.5°, 107.9° were respectively obtained. It should be noted that increasing SPAM concentration from 5000 to 10,000 ppm resulted in more reduction in the contact angle values for all smart water-polymer solutions. However, the wettability remained unchanged by increasing SPAM concentration. For example, as for SW2Mg, although increasing SPAM concentration reduced the contact angle value by 10.5°, it did not affect the neutral-wet wettability condition.

According to the total acid and base numbers of crude oil used in this study (as shown in Table 1), both carboxylic ($-COO^-$) and amine ($-NH^+$) groups are present as surface-active agents in oil. Therefore, these surface-active agents can be adsorbed on the carbonate surface in the course of making the thin sections oil-wet [64]. In the presence of divalent ions alongside SPAM polymer, $-COO^-$ and $-NH^+$ can be detached from the surface, causing it to become less oil-wet. In this regard, numerous mechanisms may contribute to wettability alteration and contact angle reduction in the combination of smart water and SPAM polymer. As for SO_4^{2-}, owing to its intrinsic negative charge, it can directly interact with $-NH^+$ via ion-dipole interaction and detach oil molecules containing amine groups from the carbonate surface [29]. Additionally, positive charges of the carbonate surface are declined in the presence of SO_4^{2-}. In other words, sulfate ions can get adsorbed on the surface through electrostatic forces and reduce the amount of positive charge on the rock surface. As a result, $-COO^-$ can be released from the carbonate surface and the wettability shifts toward less hydrophobic conditions [65]. Also, as the carbonate surface positive charge declines, repulsive forces between divalent cations and the surface are reduced. Thus, this reduction can facilitate the access of Ca^{2+} and Mg^{2+} to the rock surface to detach oil molecules containing carboxylic groups [66].

Regarding Ca^{2+} and Mg^{2+}, multi-ion exchange could be the primary mechanism leading to wettability alteration [67]. Indeed, when carboxylic groups get adsorbed on the carbonate surface, a complex structure is formed between $-COO^-$ and Ca^{2+}. In the presence of divalent cations, the $Ca^{2+}/-COO^-$ complexes can be replaced by Mg^{2+} ions, and this, in turn, can make the carbonate surface less oil-wet. In addition, due to their positive charge, Ca^{2+} and Mg^{2+} are able to diminish the negative charges present on the carbonate surface, leading to the detachment of $-NH^+$. Simply put, divalent cations can react with negatively charged carbonate species to render the surface more positively charged. Accordingly, the attractive forces between amine groups and the carbonate surface can be reduced, $-NH^+$ is released from the surface, and the wettability changes. Besides, the solubility of oil molecules containing carboxylic groups can be enhanced in the aqueous phase since divalent cations are likely to interact with $-COO^-$ [68]. As a consequence, the detachment of carboxylic groups from the carbonate rock occurs. Furthermore, divalent cations can form ion-pair with SO_4^{2-} ions [29,66]. Upon adsorption of SO_4^{2-} on the rock surface, the positive charge is reduced, and divalent cations, including Mg^{2+} and Ca^{2+}, are more likely to approach the surface. As a result, Mg^{2+} and Ca^{2+} ions can directly interact with negatively charged oil components on the carbonate surface to release them.

SPAM polymer has negative charges on its backbones owing to the presence of sulfonate groups ($-SO_3^-$). It is proposed that the

SPAM can reduce the contact angle values via the adsorption on the carbonate surface and decline the surface rock positive charge. In other words, interactions between $-SO_3^-$ on the SPAM structure and the positive charge on the carbonate rock make the polymer get adsorbed. As a result, the amount of positive charge diminishes, and oil molecules with carboxylic groups can be separated from the carbonate surface, rendering it less oil-wet. Moreover, it is possible that the charge-charge interactions allow $-SO_3^-$ to interact directly with oil molecules containing amine groups and detach them from the carbonate surface. As illustrated in Fig. 6, the excess amount of Ca^{2+}, Mg^{2+}, and SO_4^{2-} decreased the contact angle by 10.1°, 28.4°, and 6°, respectively, as the smart water was combined with 5000 ppm SPAM. It is clear that a 2 times increase in the concentration of SO_4^{2-} underperformed as opposed to that of Ca^{2+} and Mg^{2+}. Also, the same trend can be seen for smart waters containing 10,000 ppm SPAM. It is worth mentioning that the addition of each divalent ion to the smart water-polymer solution can positively or negatively affect the performance of SPAM in contact angle reduction. In the case of SO_4^{2-}, as stated earlier, it can decrease the positive charge on the carbonate surface, which could hinder the adsorption of some SPAM molecules. To put it differently, the higher the amount of SO_4^{2-} is, the more negative the carbonate surface charge will be, resulting in a reduction in the SPAM adsorption. Thus, the excess amount of SO_4^{2-} does not aid the SPAM in changing the rock wettability. Conversely, the extra amount of Ca^{2+} and Mg^{2+} can facilitate the SPAM adsorption on the rock surface, shifting the wettability toward a less oil-wet state. This is because divalent cations are capable of inducing more positive charges on the carbonate surface. Hence, more negatively charged SPAM molecules might be adsorbed on the surface to separate oil molecules from it.

3.3. Impact of divalent ions on rock/brine zeta potential

In this study, the rock/brine zeta potential values were measured to witness the effect of different smart water-polymer solutions on the carbonate surface charge, and Fig. 7 shows the obtained results. It should be highlighted that positively and negatively charged species at the carbonate rock surface, including Ca^{2+}, $CaHCO_3^+$, $CaOH^+$, HCO_3^-, and CO_3^{2-}, affect the surface charge [69]. Based on the concentrations of these charged species, the carbonate surface can have a positive or negative charge. When the positively charged surface sites dominate the carbonate surface, the surface charge becomes positive and vice versa. The presence of divalent ions and polymer can either decrease or increase the concentrations of the mentioned charged species, changing the rock/brine zeta potential value.

In the absence of SPAM polymer, the zeta potential of 2.4 mV was obtained for SW because the sum of divalent cations concentrations is higher than the concentration of SO_4^{2-}, according to Table 2. Additionally, when the SPAM was added to SW at a 5000 ppm concentration, the zeta potential decreased from 2.4 to -12.1 mV, indicating that the presence of this polymer could induce a more negative charge on the carbonate surface. Also, increasing SPAM concentration to 10,000 ppm led to a further reduction in zeta potential value. The reason for this reduction in the presence of polymer could be that SPAM can react with Ca^{2+}, $CaHCO_3^+$, and $CaOH^+$ at the surface to neutralize them. As a result, the positively charged sites decrease, making the carbonate surface charge more negative.

In addition, at 5000 ppm SPAM solution, a two-fold increase in the concentration of Ca^{2+}, Mg^{2+}, and SO_4^{2-} altered the zeta potential value from -12.1 to −10.8, 4.2 and -19.6 mV, respectively. The excess amount of Ca^{2+} and Mg^{2+} can reduce the negative charge on the carbonate surface; However, adding SO_4^{2-} to the smart water-polymer solution leads to more negative zeta potentials. Indeed, the divalent cations tend to interact with HCO_3^- and CO_3^{2-}, and consequently, the negative surface charge declines, leading to positive zeta potential. As for SO_4^{2-}, positively charged sites can be neutralized by sulfate ions, and this, in turn, makes the zeta potential more negative. It should be noted that Mg^{2+} acted better in rendering the carbonate surface more positively charged. This is because more amount of Mg^{2+} is present in smart water-polymer solutions compared to Ca^{2+}. Thus, as the Mg^{2+} concentration is increased 2 times, more negatively charged sites can be influenced, thereby changing the zeta potential to more positive values. To be more specific, the initial concentrations of Mg^{2+} and Ca^{2+} in SW are 3484 and 439.8 ppm, respectively. Doubling the concentration of Mg^{2+} yields a higher resulting concentration (6968 ppm) than doubling the concentration of Ca^{2+} (879.6 ppm). Thus, the higher Mg^{2+} concentration in SW2Mg disrupts the balance between divalent anions and cations, leading to a significant Mg^{2+} adsorption on the carbonate surface. This can be attributed to the stronger interactions within the stern layer and enhanced chemical interactions between negatively charged surface species and Mg^{2+} ions. Consequently, the site density of negatively charged species on the surface is likely reduced as the substantial presence of Mg^{2+} ions neutralizes these negatively charged species, resulting in positive zeta potential values. In contrast, the concentration of Ca^{2+} in SW2Ca is insufficient to compete with SO_4^{2-} and SPAM polymer and make the zeta potential positive.

As opposed to SW + 5000 ppm SPAM, the zeta potential was found to be -17.5, 1.1, and -26.2 mV for SW2Ca, SW2Mg, and $SW2SO_4$, respectively, with increasing polymer concentration to 10,000 ppm. It is obvious that the positive charge of the carbonate surface can be diminished by rising SPAM concentration in SW spiked with divalent ions. In the case of increasing divalent ions concurrently in 5000 ppm of SPAM, the zeta potential decreased to 0.8 and 5.9 mV for $SW2Mg_2SO_4$ and $SW2Mg_2Ca$, respectively. As is evident, the carbonate surface becomes more positively charged as Ca^{2+} and Mg^{2+} concentrations increase. This is because the site density of negatively charged species is more declined as Ca^{2+} and Mg^{2+} ions are added to the solution simultaneously.

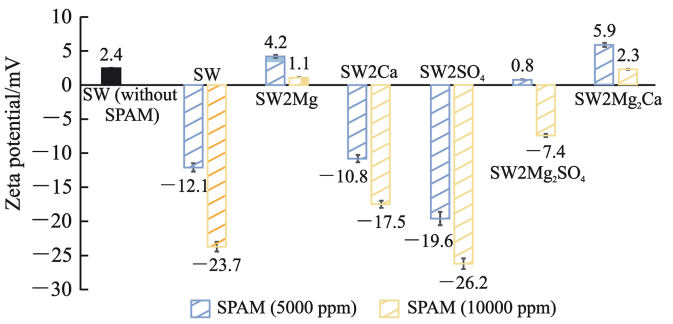

Fig. 7. Effect of different smart water-polymer solutions on rock/brine zeta potential.

3.4. Impact of divalent ions on SPAM adsorption

According to the studies of Sodeifian et al. [70] and Zhang and Seright [71], above a concentration of 3000 ppm, SPAM polymer is in a concentrated regime in which the adsorption on the rock does not depend on the polymer concentration. In other words, increasing SPAM concentration in the concentrated region does not change the polymer adsorption. Therefore, since selected SPAM concentrations were 5000 and 10,000 ppm in this study, we only measured the SPAM adsorption at 5000 ppm concentration. Fig. 8 shows the adsorption of SPAM in the presence of

different smart waters. For SW, the adsorption of 6.3 mg/g was obtained. A two-fold increase in the concentrations of Ca^{2+} and Mg^{2+} raised the adsorption to 6.7 and 9.2 mg/g, respectively. Besides, as the concentration of SO_4^{2-} was increased 2 times, the adsorption was reduced to 5.2 mg/g. Thus, as compared to divalent anions, the excess amounts of divalent cations can lead to an increase in the adsorption of SPAM. Additionally, as the excess amount of SO_4^{2-} was added to SW2Mg, the SPAM adsorption declined from 9.2 to 7.1 mg/g, indicating that sulfate ions could prevent some SPAM molecules from getting adsorbed on the carbonate rock. Nevertheless, there was a significant increase in the SPAM adsorption with the addition of Ca^{2+} to SW2Mg, raising it to 16.6 mg/g.

Generally, two prime mechanisms may account for SPAM adsorption on the carbonate rock, involving hydrogen bonding and electrostatic interactions [72,73]. Firstly, hydrogen bonds can be created between oxygen or nitrogen atoms in SPAM chains and hydrogen atoms of charged species on carbonate rock, causing the SPAM molecules to adsorb. Secondly, owing to the presence of $-SO_3^-$ on SPAM chains and charged sites at the carbonate surface, the negatively charged SPAM molecules can be attracted to the Ca^{2+}, $CaHCO_3^+$, and $CaOH^+$ via electrostatic attraction forces. As a result, the SPAM adsorption on the rock occurs. Among these two mentioned mechanisms, the electrostatic interactions could be affected positively or negatively by the presence of divalent ions, as shown in Fig. 9. As for divalent cations, Ca^{2+} and Mg^{2+} tend to neutralize the negatively charged sites at the carbonate surface and make the surface charge more positive. Therefore, SPAM molecules are more likely to readily reach the carbonate surface and get adsorbed on it due to reduced repulsive forces between negatively charged sites and $-SO_3^-$. As illustrated in Fig. 8, the addition of divalent cations to SW can increase the adsorption of polymer to a great extent, and this is because Ca^{2+} and Mg^{2+} have enough capacity to facilitate SPAM adsorption on the carbonate rock by virtue of rendering the carbonate surface charge more positive. This explanation is in line with the zeta potential results, indicating that divalent cations reduce the negative charge of carbonate rock.

In the case of divalent anions, the adsorption of SPAM on the carbonate surface can be diminished since the extra amount of SO_4^{2-} disrupts the interactions between $-SO_3^-$ from the SPAM backbones and positively charged species from the carbonate surface. To put it differently, the number of positively charged sites on the carbonate surface declines with increasing concentration of SO_4^{2-} in smart water-polymer solutions. Hence, the carbonate surface charge becomes more negative, and the SPAM adsorption reduces. This is due to the fact that repulsive forces between SPAM molecules and the carbonate surface heighten, and, as a result, less amount of polymer has a chance to be adsorbed on the surface via the mechanism of the electrostatic interactions. It is apparent that this mentioned effect of SO_4^{2-} is the reason for the reduced amount of adsorbed SPAM molecules in $SW2Mg_2SO_4$ as opposed to SW2Mg. It should be noted that the zeta potential results in this study approved the SO_4^{2-} effect on the carbonate surface charge.

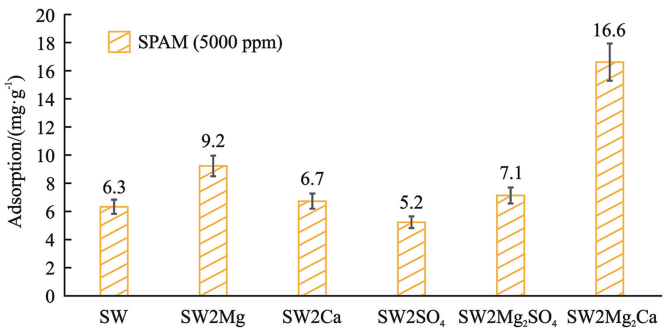

Fig. 8. Effect of different smart waters on SPAM adsorption.

3.5. Impact of smart water-polymer solutions on W/O emulsion

In this study, the emulsion experiment was performed to discern the effects of various smart waters and SPAM polymer on W/O emulsions. Fig. 10 shows the mean droplet size for different smart water-polymer solutions. As can be seen, the mean droplet size for SW without SPAM polymer was 0.048 mm. As the SPAM concentration increased to 5000 and 10,000 ppm in SW, the mean droplet size was 0.115 and 0.131 mm, respectively. Thus, the presence of SPAM polymer and increasing its concentration can heighten the size of water droplets in W/O emulsions. In general, the size of water droplet in W/O emulsions is highly dependent on the presence of surface-active agents of oil at oil/brine interface [74]. To be more specific, as more surface-active agents come to the interface, the droplet size decreases and the emulsion has more stability. On the contrary, there can be less repulsive forces between water droplets when the surface-active agents migrate from the interface to the balk of oil. As a result, the emulsion droplet size becomes larger, and the stability can be impaired. It should be highlighted that asphaltene and resin are surface-active agents present in the oil due to their molecular structures. In other words, these two oil components comprise heteroatoms and non-polar hydrocarbons making them act like surface-active agents [75]. According to the open literature, both positive and negative polar sites are present on the structures of surface-active agents. In terms of polar sites activity, negatively charged sites on asphaltene and resin are far more active than positively charged sites at fluid/fluid and rock/fluid interactions [76]. As stated earlier, the presence of SPAM polymer in SW increased the mean droplet size of water in W/O emulsion. This can be due to the fact that SPAM molecules have negative charges and cause some asphaltenes to leave the oil/brine interface. Thus, the size of water droplets increases. In other words, the negative polar sites of asphaltenes and negatively charged polymer molecules repel each other at the interface. As a result, some asphaltenes get back to the oil phase, making the water droplet size larger in W/O emulsions. Additionally, a salt-out effect may take place as SPAM polymer is added to SW. To put it differently, according to the salt-out effect, the solubility of surface active agents at the oil/brine interface decreases in the water phase, and these agents tend to move back to the oil phase [77–79]. Thus, in SW, negatively charged SPAM polymers at the oil/brine interface may hinder the solubility of asphaltenes and resins into the brine and cause the surface active agents to migrate from the interface, thereby increasing the water droplet size.

As the concentration of Ca^{2+} increased two times in SW, the mean droplet size decreased to 0.092 and 0.114 mm for SPAM concentrations of 5000 and 10,000 ppm, respectively. Indeed, doubling the Ca^{2+} in SW can attract more asphaltene molecules to the interface, resulting in more reduction in the water droplet size. Moreover, it is possible that doubling the concentration of Ca^{2+} in SPAM solution may lead to a salt-in effect. In this regard, the excess amounts of Ca^{2+} can enhance the solubility of polar oil components at the oil/brine interface and decrease the size of water droplets in the produced emulsions [80,81]. In contrast, a two-time increase in the concentration of Mg^{2+} or SO_4^{2-} led to an increase in the mean droplet size. As for Mg^{2+}, since high amounts of Mg^{2+} are present in the SW, the salting-out effect could happen at the oil/brine interface by doubling its concentration. Indeed, the solubility of oil components (e.g., asphaltenes) decreases as the concentration of Mg^{2+} is doubled. Thus, the asphaltenes tend to migrate from the interface to the oil phase. Consequently, the droplet size becomes

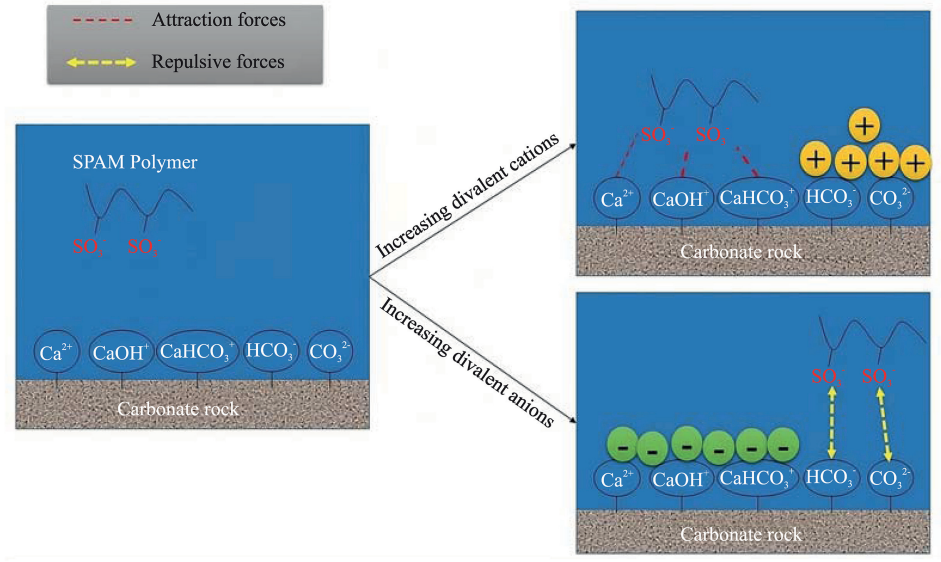

Fig. 9. Schematic of SPAM adsorption on the rock in the presence divalent ions.

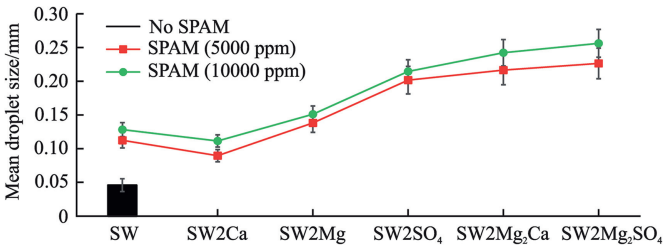

Fig. 10. Mean droplet size of produced emulsions by smart water-polymer solutions.

larger due to decreased asphaltene molecules at the interface. Also, increasing SO_4^{2-} concentration in SW can diminish the presence of asphaltenes at the interface. This is because the asphaltenes are depleted at the interface owing to the repulsive forces between SO_4^{2-} ions and negatively charged oil components. Therefore, the size of water droplets in W/O emulsion increases. In the case of increasing concentrations of two divalent ions simultaneously in smart water-polymer solutions, it is apparent that larger droplets can be seen for $SW2Mg_2SO_4$ compared to $SW2Mg_2Ca$. According to Table 2, the ionic strength of $SW2Mg_2SO_4$ is greater than that of $SW2Mg_2Ca$. As a result, the salting-out effect is more significant in $SW2Mg_2SO4$, leading to a larger mean droplet size. The images of produced emulsions for different hybrid solutions are illustrated in Fig. S3 (See supporting information).

3.6. Impact of smart water-polymer flooding on EOR

The calcite-coated micromodel flooding was conducted for SW, SW2Mg, and $SW2Mg_2SO_4$. Indeed, since among studied solutions, only SW2Mg and $SW2Mg_2SO_4$ altered the wettability to neutral-wet conditions, they were chosen for flooding experiments, and their results were compared with SW. Besides, 5000 ppm of polymer concentration was used to perform flooding tests, and we omitted the smart water-polymer solutions that contain 10,000 ppm of SPAM. This is because it may not be economically feasible to use 10,000 ppm SPAM for the EOR purpose. Apart from an economic point of view, it is crystal clear that high polymer concentration can result in the injectivity problems [82].

Following flooding experiments, the amount of oil recovery was obtained at different injected pore volumes, and the results are presented in Fig. 11. As can be seen, the ultimate oil recovery was found to be 34.2%, 36.5%, and 40.7% for SW, $SW2Mg_2SO_4$, and SW2Mg, respectively. The highest oil recovery was achieved as the concentration of Mg^{2+} was increased 2 times. Compared to SW, the reason for the 6.5% increase in the oil recovery is that SW2Mg has the highest viscosity value among studied solutions and shifts the carbonate wettability toward a more water-wet condition. Therefore, it has more potential to overcome capillary forces in the pores and throats of the micromodel, resulting in less residual oil saturation. Also, as both Mg^{2+} and SO_4^{2-} concentrations rose in the SW, the oil recovery marginally improved (2.3%). It should be mentioned that SW2Mg and $SW2Mg_2SO_4$ lead to a neutral-wet condition regarding wettability alteration. However, $SW2Mg_2SO_4$ has a lower viscosity; thus, it has less capacity to improve displacement efficiency relative to SW2Mg. Table 6 displays the breakthrough time for the hybrid fluids used for micromodel flooding. In SPAM concentration of 5000 ppm, the breakthrough time for SW, $SW2Mg_2SO_4$, and SW2Mg was found to be 111, 116, and 127 min, respectively. Indeed, SW2Mg postponed the breakthrough time more than SW and $SW2Mg_2SO_4$. This could be rooted in the fact that since the hybrid fluid of SW2Mg can alter the wettability to neutral-wet conditions and has higher viscosity, it can better overcome capillary pressure, penetrating into the pores and throats. As a result, the breakthrough time of SW2Mg increases.

The macroscopic and microscopic images of the micromodel following 1 pore volume of injected fluid are presented in Fig. 12. As for SW (Fig. 12(a)), the fingering problem can be seen. However, according to Fig. 12(b) and (c), SW2Mg and $SW2Mg_2SO_4$ reduce the viscous fingering effect, making the oil displacement more piston-like. To put it differently, the fronts of SW2Mg and $SW2Mg_2SO_4$ showed more piston-like motion, leading to more oil production. At the pore scale, oil-in-water (O/W) emulsions are seen for SW, SW2Mg, and $SW2Mg_2SO_4$ injections. In SW2Mg flooding, the number of large O/W emulsion drops increases, whereas SW injection shows numerous small-scale O/W emulsions. Not surprisingly, no water-in-oil (W/O) emulsions are present in the pores and throats of the micromodel.

Regarding wettability alteration, in some parts of the pore walls for all injections, it can be witnessed that oil layers are not present,

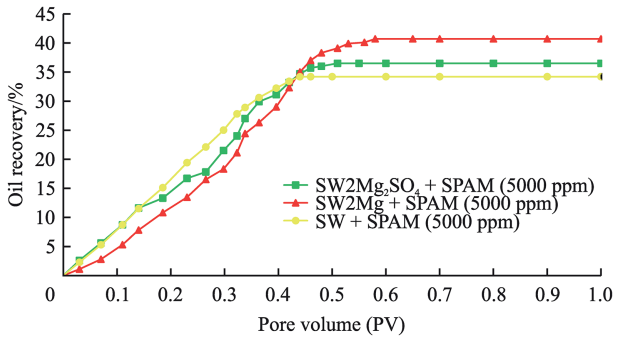

Fig. 11. Amount of oil recovery versus pore volume of injected smart water-polymer solution.

Table 6
Breakthrough time for hybrid fluids used in micromodel flooding.

Hybrid Fluid	Breakthrough Time (minutes)
SW + 5000 ppm SPAM	111
$SW2Mg_2SO_4$ + 5000 ppm SPAM	116
SW2Mg + 5000 ppm SPAM	127

making the pores water-wet. This observation contradicts the results of the contact angle test. In other words, contact angle experiments revealed that the wettability could change to neutral-wet conditions by using smart water-polymer solutions. However, the micromodel flooding showed that the pores and throats of the micromodel became water-wet in some areas. This contradiction may lie in the fact that real reservoir rock, composed of different minerals, was used in the contact angle tests, which might have different effects on changing the wettability compared to pure calcite. In other words, the micromodel was made calcite-coated by growing pure calcite layers on the pores. Thus, the presence and absence of other minerals in the rock thin sections could lead to varied results regarding wettability alteration. In this regard, Alsofi et al. [42] used pure calcite pellet and carbonate rock to evaluate wettability alteration as low salinity water and polymer were combined. They showed that the wettability changed to neutral-wet and water-wet states for the reservoir rock and calcite pellet, respectively. In this study, to better understand the mentioned contradiction, we first made calcite chips comprised of high amounts of $CaCO_3$ oil-wet and then assessed the wettability alteration. As is shown in Table 7, the wettability of used rock chips changes from oil-wet to water-wet in SW, SW2Mg, and $SW2Mg_2SO_4$. Therefore, it is sensible that some pores in the micromodel become water-wet as they are coated with pure calcite layers.

It is imperative to analyze the results of contact angle, rock/brine zeta potential, and polymer adsorption experiments concurrently to gain a deeper understanding of the impacts of potential determining ions on SPAM performance during smart water-polymer flooding. As can be seen from Figs. 6–8, a double increase in

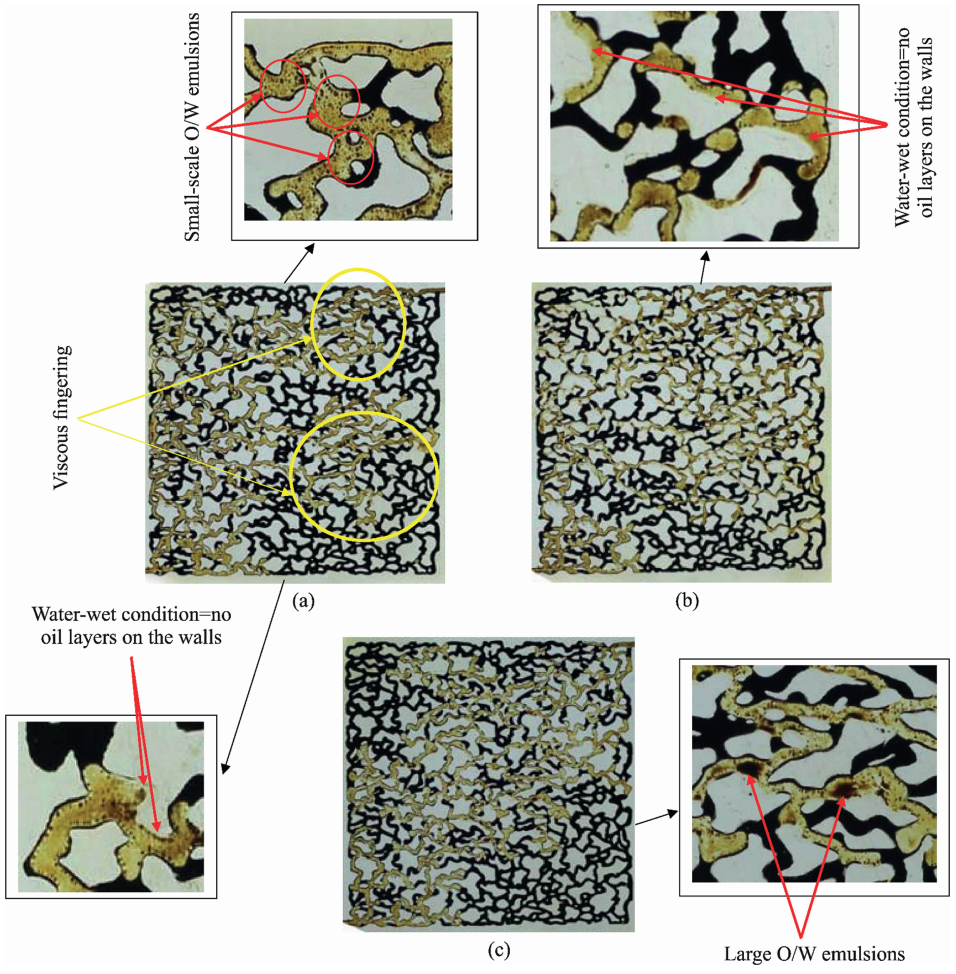

Fig. 12. Macroscopic and microscopic images of micromodel at 1 pore volume of injected smart water-polymer solution: (a) SW, (b) SW2Mg, and (c) SW2Mg2SO4.

Table 7
Effect of smart water-polymer solutions on the wettability of calcite surface.

Initial wettability condition (oil droplet)	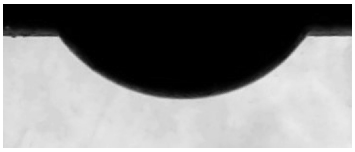	
Contact angle, degree	124 ± 3	
Smart water	Contact angle, degree	Oil droplet shape
SW	56.3 ± 2	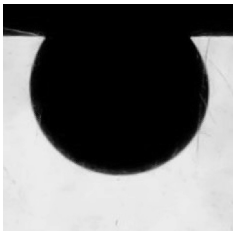
SW2Mg	28.7 ± 2	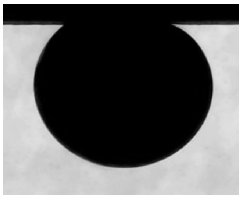
$SW2Mg_2SO_4$	35.4 ± 2	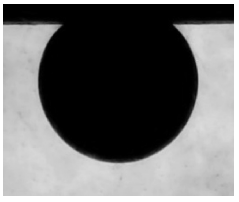

Mg^{2+} concentration in the SPAM solution can render the carbonate surface positively charged. This positive surface charge can influence both polymer adsorption and wettability alteration. Indeed, the positive carbonate surface charge can increase the adsorption of SPAM due to the enhanced electrostatic attraction forces, and, as a result, the surface can become more hydrophilic. However, increased adsorption of SPAM on the carbonate rock due to the adjustment of Mg^{2+} concentration may result in a loss of SPAM polymer during smart water-polymer flooding. This loss can, in turn, adversely affect the sweep efficiency and viscosity. The calcite-coated micromodel flooding experiments in this study suggest that SPAM adsorption might not be problematic regarding viscosity reduction, as SW2Mg flooding leads to higher oil production than SW in the presence of SPAM. For future studies, it is highly recommended to perform core flooding tests to examine both polymer adsorption and degradation in the reservoir conditions because the results of flooding in this research did not demonstrate the adverse effect of tuning Mg^{2+} concentration on ultimate oil recovery. It should be highlighted that while adjusting SO_4^{2-} concentration made the carbonate surface more negatively charged and reduced SPAM adsorption, the oil-wet wettability did not shift. Thus, tuning SO_4^{2-} concentration in SPAM solution may not be a decent option to increase oil recovery.

4. Conclusions

For the first time, seawaters, spiked with potential determining ions, were combined with SPAM polymer to boost EOR. In this regard, contact angle, zeta potential, viscosity, static adsorption, emulsion formation, and calcite-coated micromodel flooding experiments were carried out. The following are the main results of these tests:

(1) In the presence of SPAM polymer, the reduction in contact angle values followed the order: $SO_4^{2-} < Ca^{2+} < Mg^{2+}$. Although increasing SPAM concentration in smart water-polymer solutions led to a reduction in contact angle values, the overall wetting conditions of the carbonate rock remained unchanged.
(2) Among the studied potential determining ions, only the excess amount of Mg^{2+} in smart water-polymer solutions could shift the wettability from oil-wet to neutral-wet.
(3) The addition of SPAM polymer to SW induced a more negative charge on the carbonate rock. This is because SPAM molecules, due to their negative charges, tend to neutralize the positively charged species of carbonate surface (Ca^{2+}, $CaHCO_3^+$, and $CaOH^+$), and the rock/brine zeta potentials become more negative.
(4) Doubling the concentrations of Ca^{2+} and Mg^{2+} increased the adsorption of SPAM on the carbonate rock. Nevertheless, the addition of SO_4^{2-} to the smart water-polymer solution rendered the carbonate surface charge more negative. As a result, the repulsive forces between SPAM molecules and the carbonate surface increased, reducing the adsorption value.
(5) At a SPAM concentration of 5000 ppm, adding potential determining ions to the solutions marginally enhanced the viscosity due to the shielding effect and the chain entanglements. However, at the higher SPAM concentration (10,000 ppm), the excess amount of SO_4^{2-} could enhance the

viscosity from 14.4 to 15.7 cP, although the divalent cations reduced the viscosity values.

(6) The presence of SPAM polymer in smart water increased the mean water droplet size in W/O emulsions owing to the salt-out effect. Among divalent ions, only increasing Ca^{2+} concentration in a smart water-polymer solution diminished the mean droplet size.

(7) The ultimate oil recovery (at 5000 ppm of SPAM) was found to be 34.2%, 36.5%, and 40.7% for SW, SW2Mg$_2$SO$_4$, and SW2Mg, respectively. These values indicate that it is possible to adjust the concentrations of potential determining ions in seawater-polymer solution and increase the amount of oil recovery.

(8) For future studies, it is highly recommended to elucidate the impacts of potential determining ions on the performance of cationic and nonionic polymers during smart water-polymer flooding. Based on this study, the most effective approach to boost oil recovery from carbonate reservoirs and improve the performance of anionic polymers (e.g., SPAM) for EOR purposes is to optimize Mg^{2+} concentration in the seawater-polymer solution. In addition, it would be beneficial to conduct core flooding tests that examine both polymer adsorption and degradation under reservoir conditions. This recommendation is made because the current study's findings did not show any adverse effects of adjusting Mg^{2+} concentration on ultimate oil recovery, highlighting the need for further exploration of these factors.

CRediT authorship contribution statement

Seyed Masoud Ghalamizade Elyaderani: Writing – review & editing, Writing – original draft, Visualization, Validation, Methodology, Investigation, Formal analysis, Conceptualization. **Amir Hossein Saeedi Dehaghani:** Writing – review & editing, Supervision, Resources, Project administration, Methodology, Conceptualization. **Javad Razavinezhad:** Writing – review & editing, Visualization, Validation, Methodology, Investigation, Formal analysis. **Rasoul Tanhay Choshali:** Validation, Methodology, Investigation, Formal analysis.

Declaration of competing interest

The authors declare that they have no known competing financial interests or personal relationships that could have appeared to influence the work reported in this paper.

Appendix A. Supplementary data

Supplementary data to this article can be found online at https://doi.org/10.1016/j.petlm.2024.12.002.

References

[1] P. Dong, M. Puerto, G. Jian, K. Ma, K. Mateen, G. Ren, G. Bourdarot, D. Morel, M. Bourrel, S.L. Biswal, G. Hirasaki, Low-IFT foaming system for enhanced oil recovery in highly heterogeneous/fractured oil-wet carbonate reservoirs, SPE J. 23 (6) (2018) 2243–2259.

[2] H. Esfandyari, A. Moghani Rahimi, F. Esmaeilzadeh, A. Davarpanah, A.H. Mohammadi, Amphoteric and cationic surfactants for enhancing oil recovery from carbonate oil reservoirs, J. Mol. Liq. 322 (2021) 114518.

[3] B. Hou, R. Jia, M. Fu, Y. Wang, C. Jiang, B. Yang, Y. Huang, Wettability alteration of oil-wet carbonate surface induced by self-dispersing silica nanoparticles: mechanism and monovalent metal ion's effect, J. Mol. Liq. 294 (2019) 111601.

[4] S. Sakthivel, M. Elsayed, Enhanced oil recovery by spontaneous imbibition of imidazolium based ionic liquids on the carbonate reservoir, J. Mol. Liq. 340 (2021) 117301.

[5] P. Barreau, H. Bertin, D. Lasseux, P. Giénat, A. Zaitoun, Water control in producing wells: influence of an adsorbed-polymer layer on relative permeabilities and capillary pressure, SPE Reservoir Eng. 12 (4) (1997) 234–239.

[6] A.M. Selem, N. Agenet, Y. Gao, A.Q. Raeini, M.J. Blunt, B. Bijeljic, Pore-scale imaging and analysis of low salinity waterflooding in a heterogeneous carbonate rock at reservoir conditions, Sci. Rep. 11 (1) (2021) 15063.

[7] J. Lu, A. Goudarzi, P. Chen, D.H. Kim, M. Delshad, K.K. Mohanty, K. Sepehrnoori, U.P. Weerasooriya, G.A. Pope, Enhanced oil recovery from high-temperature, high-salinity naturally fractured carbonate reservoirs by surfactant flood, J. Petrol. Sci. Eng. 124 (2014) 122–131.

[8] R. Rostami Ravari, S. Strand, T. Austad, Combined surfactant-enhanced gravity drainage (SEGD) of oil and the wettability alteration in carbonates: the effect of rock permeability and interfacial tension (IFT), Energy Fuels 25 (5) (2011) 2083–2088.

[9] M. AfzaliTabar, A. Rashidi, M. Alaei, H. Koolivand, S. Pourhashem, S. Askari, Hybrid of quantum dots for interfacial tension reduction and reservoir alteration wettability for enhanced oil recovery (EOR), J. Mol. Liq. 307 (2020) 112984.

[10] E. Jafarbeigi, E. Kamari, F. Salimi, A. Mohammadidoust, Experimental study of the effects of a novel nanoparticle on enhanced oil recovery in carbonate porous media, J. Petrol. Sci. Eng. 195 (2020) 107602.

[11] I. Raj, M. Qu, L. Xiao, J. Hou, Y. Li, T. Liang, T. Yang, M. Zhao, Ultralow concentration of molybdenum disulfide nanosheets for enhanced oil recovery, Fuel 251 (2019) 514–522.

[12] B. Sami, A. Azdarpour, B. Honarvar, M. Nabipour, A. Keshavarz, Application of a novel natural surfactant extracted from Avena Sativa for enhanced oil recovery during low salinity water flooding: synergism of natural surfactant with different salts, J. Mol. Liq. 362 (2022) 119693.

[13] A. Bera, S. Shah, M. Shah, J. Agarwal, R.K. Vij, Mechanistic study on silica nanoparticles-assisted guar gum polymer flooding for enhanced oil recovery in sandstone reservoirs, Colloids Surf. A Physicochem. Eng. Asp. 598 (2020) 124833.

[14] R. Elhaei, R. Kharrat, M. Madani, Stability, flocculation, and rheological behavior of silica suspension-augmented polyacrylamide and the possibility to improve polymer flooding functionality, J. Mol. Liq. 322 (2021) 114572.

[15] A. Esfandiarian, A. Maghsoudian, M. Shirazi, Y. Tamsilian, S. Kord, J.J. Sheng, Mechanistic investigation of the synergy of a wide range of salinities and ionic liquids for enhanced oil recovery: fluid–fluid interactions, Energy Fuels 35 (4) (2021) 3011–3031.

[16] H. Guo, Y. Li, D. Kong, R. Ma, B. Li, F. Wang, Lessons learned from alkali/surfactant/polymer-flooding field tests in China, SPE Reservoir Eval. Eng. 22 (1) (2018) 78–99.

[17] S.O. Olayiwola, M. Dejam, A comprehensive review on interaction of nanoparticles with low salinity water and surfactant for enhanced oil recovery in sandstone and carbonate reservoirs, Fuel 241 (2019) 1045–1057.

[18] H. Pei, G. Zhang, J. Ge, M. Tang, Y. Zheng, Comparative effectiveness of alkaline flooding and alkaline–surfactant flooding for improved heavy-oil recovery, Energy Fuels 26 (5) (2012) 2911–2919.

[19] S. Rellegadla, S. Jain, J.S. Sangwai, M. Lavania, B. Lal, L. Gieg, A. Rajasekar, A. Bera, A. Agrawal, Wettability alteration of the oil-wet carbonate by viscosity-augmented guar galactomannan for enhanced oil recovery, ACS Appl. Polym. Mater. 3 (4) (2021) 1983–1994.

[20] A. Rezaei, M. Abdi-Khangah, A. Mohebbi, A. Tatar, A.H. Mohammadi, Using surface modified clay nanoparticles to improve rheological behavior of Hydrolized Polyacrylamid (HPAM) solution for enhanced oil recovery with polymer flooding, J. Mol. Liq. 222 (2016) 1148–1156.

[21] A. Katende, F. Sagala, A critical review of low salinity water flooding: mechanism, laboratory and field application, J. Mol. Liq. 278 (2019) 627–649.

[22] J. Hao, S. Mohammadkhani, H. Shahverdi, M.N. Esfahany, A. Shapiro, Mechanisms of smart waterflooding in carbonate oil reservoirs - a review, J. Petrol. Sci. Eng. 179 (2019) 276–291.

[23] Y. Chen, Q. Xie, W. Pu, A. Saeedi, Drivers of pH increase and implications for low salinity effect in sandstone, Fuel 218 (2018) 112–117.

[24] P.I. Sagbana, K. Sarkodie, W.A. Nkrumah, A critical review of carbonate reservoir wettability modification during low salinity waterflooding, Petroleum 9 (3) (2022) 317–330.

[25] A.H. Saeedi Dehaghani, S.M. Ghalamizade Elyaderani, Application of ion-engineered Persian Gulf seawater in EOR: effects of different ions on interfacial tension, contact angle, zeta potential, and oil recovery, Petrol. Sci. 18 (3) (2021) 895–908.

[26] M.R. Zaeri, R. Hashemi, H. Shahverdi, M. Sadeghi, Enhanced oil recovery from carbonate reservoirs by spontaneous imbibition of low salinity water, Petrol. Sci. 15 (3) (2018) 564–576.

[27] R.A. Nasralla, E. Sergienko, S.K. Masalmeh, H.A. van der Linde, N.J. Brussee, H. Mahani, B.M. Suijkerbuijk, I.S. Al-Qarshubi, Potential of low-salinity waterflood to improve oil recovery in carbonates: demonstrating the effect by qualitative coreflood, SPE J. 21 (5) (2016) 1643–1654.

[28] J.J. Sheng, Critical review of low-salinity waterflooding, J. Petrol. Sci. Eng. 120 (2014) 216–224.

[29] S.M. Ghalamizade Elyaderani, A.H. Saeedi Dehaghani, J. Razavinezhad, Tuned low-salinity waterflooding in carbonate reservoirs: impact of Cr2O72-, C6H5COO-, and SO42-, SPE J. (2023) 1–14.

[30] H. Mahani, A.L. Keya, S. Berg, R. Nasralla, Electrokinetics of carbonate/brine interface in low-salinity waterflooding: effect of brine salinity, composition, rock type, and pH on ?-Potential and a surface-complexation model, SPE J. 22 (1) (2016) 53–68.

[31] M. Golmohammadi, S. Mohammadi, H. Mahani, S. Ayatollahi, The non-linear effect of oil polarity on the efficiency of low salinity waterflooding: a pore-level investigation, J. Mol. Liq. 346 (2022) 117069.
[32] P. Ahmadi, H. Asaadian, A. Khadivi, S. Kord, A new approach for determination of carbonate rock electrostatic double layer variation towards wettability alteration, J. Mol. Liq. 275 (2019) 682–698.
[33] A. Hiorth, L.M. Cathles, M.V. Madland, The impact of pore water chemistry on carbonate surface charge and oil wettability, Transport Porous Media 2010 85 (1) (2010) 1–21, 85:1.
[34] A. Maghsoudian, A. Esfandiarian, S. Kord, Y. Tamsilian, B.S. Soulgani, Direct insights into the micro and macro scale mechanisms of symbiotic effect of SO_4^{2-}, Mg^{2+}, and Ca^{2+} ions concentration for smart waterflooding in the carbonated coated micromodel system, J. Mol. Liq. 315 (2020) 113700.
[35] A.H.S. Dehaghani, M. Hosseini, A. Tajikmansori, H. Moradi, A mechanistic investigation of the effect of ion-tuned water injection in the presence of cationic surfactant in carbonate rocks: an experimental study, J. Mol. Liq. 304 (2020) 112781.
[36] S.O. Olayiwola, M. Dejam, Comprehensive experimental study on the effect of silica nanoparticles on the oil recovery during alternating injection with low salinity water and surfactant into carbonate reservoirs, J. Mol. Liq. 325 (2021) 115178.
[37] M.P. Yutkin, H. Mishra, T.W. Patzek, J. Lee, C.J. Radke, Bulk and surface aqueous speciation of calcite: implications for low-salinity waterflooding of carbonate reservoirs, SPE J. 23 (1) (2017) 84–101.
[38] Y. Zhao, S. Yin, R.S. Seright, S. Ning, Y. Zhang, B. Bai, Enhancing heavy-oil-recovery efficiency by combining low-salinity-water and polymer flooding, SPE J. 26 (3) (2021) 1535–1551.
[39] B. Shaker Shiran, A. Skauge, Enhanced oil recovery (EOR) by combined low salinity water/polymer flooding, Energy Fuels 27 (3) (2013) 1223–1235.
[40] M. Souayeh, R.S. Al-Maamari, A. Mansour, M. Aoudia, T. Divers, Injectivity and potential wettability alteration of low-salinity polymer in carbonates: role of salinity, polymer molecular weight and concentration, and mineral dissolution, SPE J. 27 (1) (2022) 840–863.
[41] Z. Li, S. Ayirala, R. Mariath, A. AlSofi, Z. Xu, A. Yousef, Microscale effects of polymer on wettability alteration in carbonates, SPE J. 25 (4) (2020) 1884–1894.
[42] A.M. AlSofi, J. Wang, A.M. AlBoqmi, M.B. AlOtaibi, S.C. Ayirala, A.A. AlYousef, Smartwater synergy with chemical enhanced oil recovery: polymer effects on smartwater, SPE Reservoir Eval. Eng. 22 (1) (2018) 61–77.
[43] Y. Lee, W. Lee, Y. Jang, W. Sung, Oil recovery by low-salinity polymer flooding in carbonate oil reservoirs, J. Petrol. Sci. Eng. 181 (2019) 106211.
[44] M. Amiri, M. Fatemi, E. Biniaz Delijani, Effect of brine salinity and hydrolyzed polyacrylamide concentration on the Oil/Brine and Brine/Rock Interactions: implications on enhanced oil recovery by hybrid low salinity polymer flooding in sandstones, Fuel 324 (2022) 124630.
[45] A. Kakati, G. Kumar, J.S. Sangwai, Low salinity polymer flooding: effect on polymer rheology, injectivity, retention, and oil recovery efficiency, Energy Fuels 34 (5) (2020) 5715–5732.
[46] E. Unsal, A.B.G.M. ten Berge, D.A.Z. Wever, Low salinity polymer flooding: lower polymer retention and improved injectivity, J. Petrol. Sci. Eng. 163 (2018) 671–682.
[47] U. Alfazazi, W. AlAmeri, M.R. Hashmet, Experimental investigation of polymer flooding with low-salinity preconditioning of high temperature–high-salinity carbonate reservoir, J. Pet. Explor. Prod. Technol. 9 (2) (2019) 1517–1530.
[48] M. Tahir, R.E. Hincapie, L. Ganzer, Influence of sulfate ions on the combined application of modified water and polymer flooding—rheology and oil recovery, Energies 13 (Issue 9) (2020).
[49] E. Hernández, E. Valero, I. Rodríguez, E. Guerra, J. Espinoza, R. Briceño, A. Veliz, Enhancing the recovery of an extra heavy oil reservoir by using low salinity polymer flooding, in: SPE Latin American and Caribbean Petroleum Engineering Conference, 2020. D011S002R003.
[50] M.B. Abdullahi, S.R. Jufar, S. Kumar, T.M. Al-shami, B.M. Negash, Synergistic effect of Polymer-Augmented low salinity flooding for oil recovery efficiency in Illite-Sand porous media, J. Mol. Liq. 358 (2022) 119217.
[51] I.D. Piñerez Torrijos, T. Puntervold, S. Strand, T. Austad, T.H. Bleivik, H.I. Abdullah, An experimental study of the low salinity Smart Water - polymer hybrid EOR effect in sandstone material, J. Petrol. Sci. Eng. 164 (2018) 219–229.
[52] R. Rahimi, A.S. Dehaghani, An experimental study on the viscosity of SPAM solutions with a new correlation predicting the apparent viscosity of sulfonated polyacrylamides, Petroleum 7 (1) (2021) 64–69.
[53] M. Rashidi, A.M. Blokhus, A. Skauge, Viscosity study of salt tolerant polymers, J. Appl. Polym. Sci. 117 (3) (2010) 1551–1557.
[54] A. Shabib-Asl, M.A. Mohammed, M. Kermanioryani, P.P.J. Valentim, Effects of low salinity water ion composition on wettability alteration in sandstone reservoir rock: a laboratory investigation, J. Nat. Sci. Res. 4 (2014) 34–41.
[55] W. Wang, S. Chang, A. Gizzatov, Toward reservoir-on-a-chip: fabricating reservoir micromodels by in situ growing calcium carbonate nanocrystals in microfluidic channels, ACS Appl. Mater. Interfaces 9 (34) (2017) 29380–29386.
[56] A. Maghsoudian, Y. Tamsilian, S. Kord, B. Soltani Soulgani, A. Esfandiarian, M. Shajirat, Styrene intermolecular associating incorporated-polyacrylamide flooding of crude oil in carbonate coated micromodel system at high temperature, high salinity condition: rheology, wettability alteration, recovery mechanisms, J. Mol. Liq. 337 (2021) 116206.
[57] A. Esfandiarian, A. Maghsoudian, A. Izadpanahi, Y. Tamsilian, S. Kord, Direct Macroscopic and Microscopic Insight to the Ionic Liquid Demulsification Process at High-Salinity and High-Temperature Conditions, 2022, 2022, pp. 1–5.
[58] L.M. Corredor, M.M. Husein, B.B. Maini, A review of polymer nanohybrids for oil recovery, Adv. Colloid Interface Sci. 272 (2019) 102018.
[59] B. Sarsenbekuly, W. Kang, H. Fan, H. Yang, C. Dai, B. Zhao, S.B. Aidarova, Study of salt tolerance and temperature resistance of a hydrophobically modified polyacrylamide based novel functional polymer for EOR, Colloids Surf. A Physicochem. Eng. Asp. 514 (2017) 91–97.
[60] A. Aguirre Giraldo, I. Moncayo-Riascos, R. Ribadeneira, Effect of the cations (Na^+, Ca^{2+}, Fe^{2+}, and Fe^{3+}) on the partially hydrolyzed polyacrylamide shrinking by molecular dynamics simulations, Energy Fuels 36 (10) (2022) 5228–5239.
[61] X. Zhang, B. Li, F. Pan, X. Su, Y. Feng, Enhancing oil recovery from low-permeability reservoirs with a thermoviscosifying water-soluble polymer, Molecules 26 (Issue 24) (2021).
[62] Y. Marcus, Ionic radii in aqueous solutions, Chem. Rev. 88 (8) (1988) 1475–1498.
[63] M. Lashkarbolooki, S. Ayatollahi, M. Riazi, Mechanistical study of effect of ions in smart water injection into carbonate oil reservoir, Process Saf. Environ. Protect. 105 (2017) 361–372.
[64] Y. Chen, A. Sari, Q. Xie, P.V. Brady, M.M. Hossain, A. Saeedi, Electrostatic origins of CO_2-increased hydrophilicity in carbonate reservoirs, Sci. Rep. 8 (1) (2018) 17691.
[65] S. Rashid, M.S. Mousapour, S. Ayatollahi, M. Vossoughi, A.H. Beigy, Wettability alteration in carbonates during "Smart Waterflood": underlying mechanisms and the effect of individual ions, Colloids Surf. A Physicochem. Eng. Asp. 487 (2015) 142–153.
[66] S.R. Moosavi, M. Rayhani, M.R. Malayeri, M. Riazi, Impact of monovalent and divalent cationic and anionic ions on wettability alteration of dolomite rocks, J. Mol. Liq. 281 (2019) 9–19.
[67] S. Bai, J. Kubelka, M. Piri, Wettability alteration by Smart Water multi-ion exchange in carbonates: a molecular dynamics simulation study, J. Mol. Liq. 332 (2021) 115830.
[68] R. Mokhtari, S. Ayatollahi, Dissociation of polar oil components in low salinity water and its impact on crude oil–brine interfacial interactions and physical properties, Petrol. Sci. 16 (2) (2019) 328–343.
[69] R.K. Saw, A. Mandal, A mechanistic investigation of low salinity water flooding coupled with ion tuning for enhanced oil recovery, RSC Adv. 10 (69) (2020) 42570–42583.
[70] G. Sodeifian, R. Daroughegi, J. Aalaie, Study of adsorptive behavior of sulfonated polyacrylamide onto carbonate rock particles to enhance oil recovery, Kor. J. Chem. Eng. 32 (12) (2015) 2484–2491.
[71] G. Zhang, R.S.S. Seright, Effect of concentration on HPAM retention in porous media, SPE J. 19 (3) (2014) 373–380.
[72] S. Al-Hajri, S.M. Mahmood, H. Abdulelah, S. Akbari, An overview on polymer retention in porous media, in: Energies, 11, 2018. Issue 10.
[73] S. Banerjee, Z.R. Abdulsattar, K. Agim, R.H. Lane, B. Hascakir, Mechanism of polymer adsorption on shale surfaces: effect of polymer type and presence of monovalent and divalent salts, Petroleum 3 (3) (2017) 384–390.
[74] M. Shafiei, Y. Kazemzadeh, D.A. Martyushev, Z. Dai, M. Riazi, Effect of chemicals on the phase and viscosity behavior of water in oil emulsions, Sci. Rep. 13 (1) (2023) 4100.
[75] R. Hamidian, M. Lashkarbolooki, H. Amani, Evaluation of surface activity of asphaltene and resin fractions of crude oil in the presence of different electrolytes through dynamic interfacial tension measurement, J. Mol. Liq. 300 (2020) 112297.
[76] A. Tajikmansori, A. Hossein Saeedi Dehaghani, S. Sadeghnejad, M. Haghighi, New insights into effect of the electrostatic properties on the interfacial behavior of asphaltene and resin: an experimental study of molecular structure, J. Mol. Liq. 377 (2023) 121526.
[77] S. Mohammadreza Shams, Y. Kazemzadeh, M. Riazi, F.B. Cortés, Effect of pressure on the optimal salinity point of the aqueous phase in emulsion formation, J. Mol. Liq. 362 (2022) 119783.
[78] M. Shafiei, Y. Kazemzadeh, G.M. Shirazy, M. Riazi, Evaluating the role of salts on emulsion properties during water-based enhanced oil recovery: ion type, concentration, and water content, J. Mol. Liq. 364 (2022) 120028.
[79] A. Khalilnezhad, H. Rezvani, P. Ganji, Y. Kazemzadeh, A Complete experimental study of oil/water interfacial properties in the presence of TiO2 nanoparticles and different ions, Oil Gas Sci. Technol. – Rev. IFP Energies Nouvelles 74 (2019).
[80] Y. Kazemzadeh, I. Ismail, H. Rezvani, M. Sharifi, M. Riazi, Experimental investigation of stability of water in oil emulsions at reservoir conditions: effect of ion type, ion concentration, and system pressure, Fuel 243 (2019) 15–27.
[81] Y. Kazemzadeh, M. Sharifi, M. Riazi, Mutual effects of Fe3O4/chitosan nanocomposite and different ions in water for stability of water-in-oil (w/o) emulsions at low–high salinities, Energy Fuels 32 (12) (2018) 12101–12117.
[82] A. Mohsenatabar Firozjaii, H.R. Saghafi, Review on chemical enhanced oil recovery using polymer flooding: fundamentals, experimental and numerical simulation, Petroleum 6 (2) (2020) 115–122.